AGU PUBLICATIONS

Geophysical Research Letters

RESEARCH LETTER
10.1002/2016GL069599

Key Points:
- Measurements of formic acid mixing ratios and eddy fluxes over a boreal forest canopy in late spring/early summer
- Bidirectional, but mostly upward formic acid fluxes suggest greatly underestimated sources, by up to a factor of 10, in the boreal forest
- Update of GEOS-Chem model reduces model bias for formic acid concentration in the boundary layer, but not in the free troposphere

Supporting Information:
- Supporting Information S1

Correspondence to:
S. Schobesberger,
sschobes@uw.edu

Citation:
Schobesberger, S., et al. (2016), High upward fluxes of formic acid from a boreal forest canopy, *Geophys. Res. Lett.*, *43*, 9342–9351, doi:10.1002/2016GL069599.

Received 17 MAY 2016
Accepted 24 AUG 2016
Accepted article online 26 AUG 2016
Published online 14 SEP 2016

High upward fluxes of formic acid from a boreal forest canopy

Siegfried Schobesberger[1,2], Felipe D. Lopez-Hilfiker[1], Ditte Taipale[3,4], Dylan B. Millet[5], Emma L. D'Ambro[6], Pekka Rantala[2], Ivan Mammarella[2], Putian Zhou[2], Glenn M. Wolfe[7,8], Ben H. Lee[1], Michael Boy[2], and Joel A. Thornton[1]

[1]Department of Atmospheric Sciences, University of Washington, Seattle, Washington, USA, [2]Department of Physics, University of Helsinki, Helsinki, Finland, [3]Department of Plant Physiology, Estonian University of Life Sciences, Tartu, Estonia, [4]Department of Forest Sciences, University of Helsinki, Helsinki, Finland, [5]Department of Soil, Water, and Climate, University of Minnesota, Minneapolis-Saint Paul, Minnesota, USA, [6]Department of Chemistry, University of Washington, Seattle, Washington, USA, [7]Atmospheric Chemistry and Dynamics Lab, NASA Goddard Space Flight Center, Greenbelt, Maryland, USA, [8]Joint Center for Earth Systems Technology, University of Maryland Baltimore County, Baltimore, Maryland, USA

Abstract Eddy covariance fluxes of formic acid, HCOOH, were measured over a boreal forest canopy in spring/summer 2014. The HCOOH fluxes were bidirectional but mostly upward during daytime, in contrast to studies elsewhere that reported mostly downward fluxes. Downward flux episodes were explained well by modeled dry deposition rates. The sum of net observed flux and modeled dry deposition yields an upward "gross flux" of HCOOH, which could not be quantitatively explained by literature estimates of direct vegetative/soil emissions nor by efficient chemical production from other volatile organic compounds, suggesting missing or greatly underestimated HCOOH sources in the boreal ecosystem. We implemented a vegetative HCOOH source into the GEOS-Chem chemical transport model to match our derived gross flux and evaluated the updated model against airborne and spaceborne observations. Model biases in the boundary layer were substantially reduced based on this revised treatment, but biases in the free troposphere remain unexplained.

1. Introduction

Carboxylic acids comprise a large fraction of atmospheric volatile organic compounds (VOC), with formic acid (HCOOH) among the most abundant. HCOOH is a common product of VOC oxidation and thus observations offer constraints on the importance of various pathways and precursors [*Millet et al.*, 2015]. HCOOH is a major source of acidity in precipitation, especially in remote areas [e.g., *Keene et al.*, 1983] and plays an important role in atmospheric aqueous-phase chemistry by affecting in-cloud hydroxyl radical (OH) concentrations [*Jacob*, 1986]. Although HCOOH is highly volatile, its solubility and ubiquitous distribution may also allow it to influence cloud drop activation and growth [*Kulmala et al.*, 1993; *Nenes et al.*, 2002].

A key unresolved issue is that atmospheric concentrations of HCOOH are often factors of 2 to 6 higher than expected from known sources and sinks [*Millet et al.*, 2015; *Paulot et al.*, 2011; *Stavrakou et al.*, 2012; *Yuan et al.*, 2015], implying strongly underestimated or missing sources, or overestimated sinks, in current budget determinations. The highest HCOOH concentrations tend to be in the planetary boundary layer over tropical and temperate forested regions, often exceeding a few parts per billion by volume (ppbv) [*Hartmann et al.*, 1991; *Hofmann et al.*, 1997; *Millet et al.*, 2015; *Seco et al.*, 2007; *Suzuki*, 1997]. The HCOOH budget discrepancy thus likely projects onto our understanding of organic multiphase photochemistry, biogenic emission inventories, and models of wet and dry deposition. Herein we focus on potential underestimates of two broad classes of HCOOH sources: direct emissions and secondary chemical production.

HCOOH is directly emitted from plant leaves and soils. Plant emissions have been measured at up to 6.5 nmol m^{-2} min^{-1} [*Kesselmeier et al.*, 1998], but are usually <1 nmol m^{-2} min^{-1} for typical daytime conditions [*Seco et al.*, 2007], with light and temperature dependencies similar to isoprene [*Guenther et al.*, 1995; *Kesselmeier et al.*, 1997]. Bacterial activity in soil is another natural source of direct HCOOH emissions. There have been few measurements of soil emissions [*Enders et al.*, 1992; *Sanhueza and Andreae*, 1991] and notably none from boreal forests, but the available literature suggests that soil-based HCOOH sources are important in areas with sparse vegetation. Other direct HCOOH emission sources are biomass and biofuel burning

[*Goode et al*., 2000], agriculture [*Ngwabie et al*., 2008], formicine ants [*Graedel and Eisner*, 1988], and fossil fuel combustion [*Glasius et al*., 2001; *Kawamura et al*., 1985; *Talbot et al*., 1988].

Secondary HCOOH sources are probably equally or more important, with chemical production contributing ~65% or more of its global budget [*Millet et al*., 2015; *Stavrakou et al*., 2012]. HCOOH formation mechanisms involve a large number of possible pathways and are far from being completely understood [*Millet et al*., 2015]. HCOOH is a photochemical oxidation byproduct of many organic precursors [*Paulot et al*., 2011; *Stavrakou et al*., 2012]. Important specific secondary sources include OH-initiated oxidation of isoprene and ozonolysis of alkenes with terminal double bonds, including isoprene, many monoterpenes, other terpenoids, and simpler alkenes such as ethene and propene. It is likely that any monoterpene or sesquiterpene will yield HCOOH upon oxidation, whether initiated by ozone (O_3) [*Lee et al*., 2006b] or OH [*Larsen et al*., 2001; *Lee et al*., 2006a].

The largest HCOOH sinks are wet and dry deposition, responsible for an estimated 73–83% of HCOOH losses globally [*Millet et al*., 2015; *Stavrakou et al*., 2012]. Together with photochemical oxidation by OH, this leads to a global HCOOH lifetime of ~4–6 days. With an effective Henry's law constant of $4–7 \times 10^6$ M atm^{-1} [*Sander*, 2015], HCOOH is promptly removed via washout during precipitation or by cloud scavenging and efficiently removed from the boundary layer via dry deposition [*Nguyen et al*., 2015]. As a result, plant leaves and soils are both sources and sinks of HCOOH, so the net flux above a forest canopy can be upward or downward.

Previous studies have investigated the interplay of HCOOH sources and sinks in forested ecosystems, mostly by measuring emission and dry deposition in branch- to plant-sized enclosures or via vertical concentration gradient measurements. Only recently has the atmosphere-ecosystem exchange of HCOOH also been studied using eddy covariance flux measurements [*Nguyen et al*., 2015]. Air-canopy HCOOH exchange has been found to be bidirectional [e.g., *Kesselmeier*, 2001], with corresponding exchange velocities (V_{ex}) between -1 cm s^{-1} and $+0.2$ cm s^{-1} for an Amazon canopy [*Kuhn et al*., 2002], savanna region [*Hartmann et al*., 1991], and southeastern U.S. temperate forest [*Nguyen et al*., 2015]. Recent modeling studies corroborate the existence of a large biogenic source of HCOOH not included in current chemistry or emission schemes in the tropics, the southeastern U.S., and boreal forests [*Millet et al*., 2015; *Stavrakou et al*., 2012]. These studies suggest yet unknown high-yield HCOOH formation pathways from oxidation of monoterpenes or other biogenic VOC, although they cannot exclude missing direct emissions.

Here we present HCOOH concentration and eddy flux measurements over a boreal forest canopy during spring/summer 2014. Boreal forests have been identified as a key region for much of the global production of HCOOH, as well as for our lack of understanding of the underlying processes. To our knowledge, these are the first direct measurements of HCOOH exchange above a boreal forest ecosystem, providing an important constraint on the boundary layer sources and sinks of HCOOH.

2. Methods

The results presented here are based on measurements at the Station for Measuring Ecosystem-Atmosphere Relations (SMEAR II) in the boreal forest in Hyytiälä, Finland, from 28 April to 3 June 2014. They were part of an extensive field campaign to study Biogenic Aerosols—Effects on Clouds and Climate (BAECC). Station and measurement environment are detailed in the Supporting Information S1 and elsewhere [e.g., *Duursma et al*., 2009; *Hari and Kulmala*, 2005; *Kulmala et al*., 2001; *Vesala et al*., 2005]. Flux measurements for this study were conducted 35 m above the forest floor from a tower. The associated flux footprint is dominated by Scots pine (*Pinus sylvestris* L.) and Norway spruce (*Picea abies* (L.) H. Karst). The SMEAR II station provides a comprehensive suite of support measurements, publicly available via the smartSMEAR website at http://avaa.tdata.fi/web/smart/smear, which we employ here for data analysis and interpretation (details in the Supporting Information S1) [*Junninen et al*., 2009; *Schuepp et al*., 1990].

The primary instruments for this study were a high-frequency (10 Hz) sonic anemometer (METEK USA-1) and an Iodide-Adduct High-Resolution Time-of-Flight Chemical Ionization Mass Spectrometer (CIMS) for simultaneous concentration measurements of HCOOH and many other compounds [*Lee et al*., 2014]. Due to the instrument operation modes using the FIGAERO inlet [*Lopez-Hilfiker et al*., 2014], fluxes were obtained for 45 min blocks separated by 1 h intervals. Instrumental sensitivity toward HCOOH was determined continuously via addition of H^{13}COOH from a gravimetrically calibrated permeation tube.

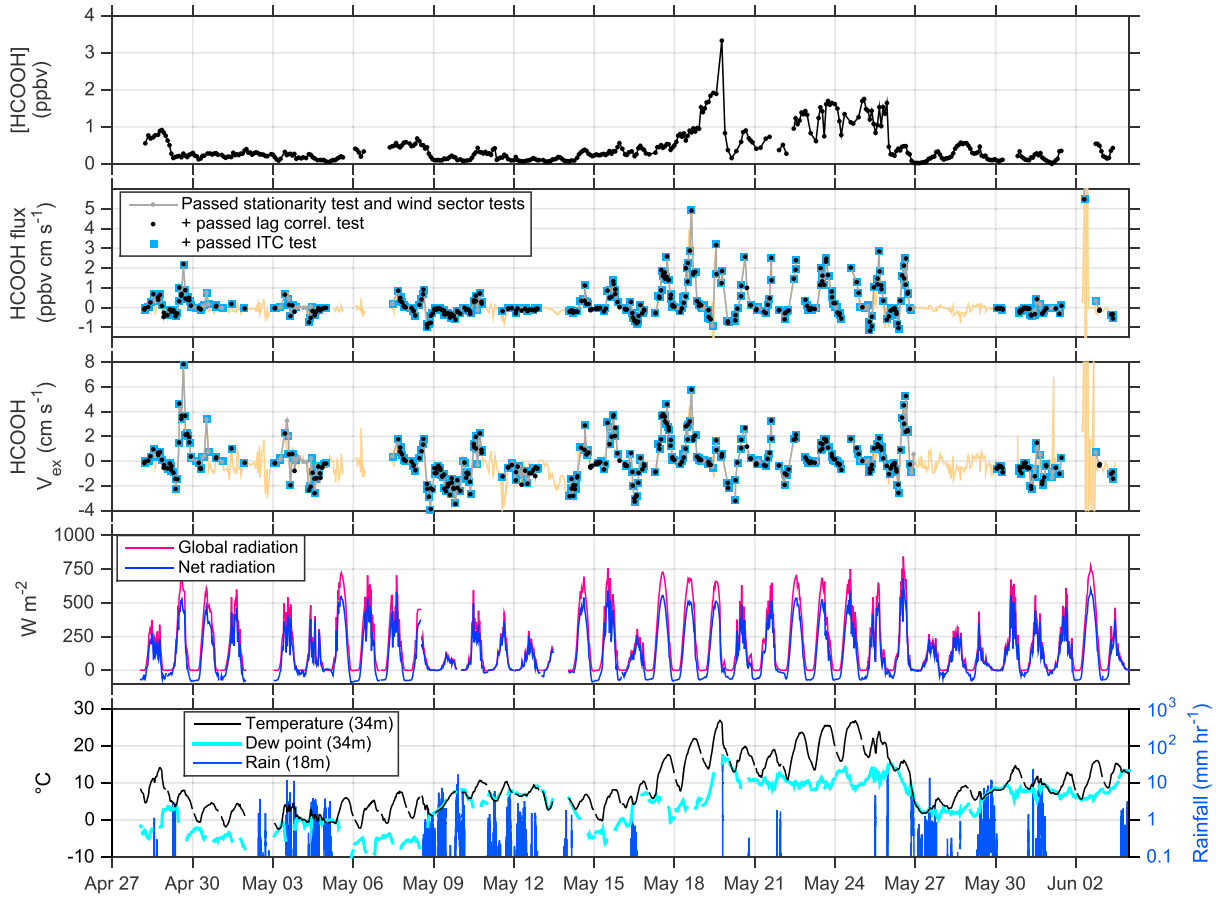

Figure 1. From top to bottom, (first panel) measured [HCOOH] (ppbv), (second panel) HCOOH flux (ppbv cm^{-1} s), (third panel) exchange velocity V_{ex} (cm s^{-1}), (fourth panel) global (short-wave) and net radiation (see Supporting Information), and (fifth panel) temperature, dew point, and precipitation intensity. All fluxes and V_{ex} are shown in orange; the subset that fulfilled various quality control criteria is highlighted in gray, black, and blue (see Supporting Information).

We followed established best practices in the subsequent eddy covariance analysis [e.g., *Farmer et al*., 2006; *Wolfe et al*., 2009]. Data with wind direction between 350° and 070° were discarded due to an obstruction to the northeast. Several quality filters were applied, viz., a stationarity test [*Foken and Wichura*, 1996], a test for clear lag correlation, and an integral turbulence characteristics test [*Rannik et al*., 2003]. Sixty-five percent of daytime and 53% of nighttime flux periods passed all those tests. Flux underestimation was typically 5%, mainly due to instrument time response. The calibration uncertainty was 22%, mainly due to variations in $H^{13}COOH$ flow. Including random instrument noise, we conservatively estimated a total measurement uncertainty of 30% for the derived HCOOH fluxes and 10% for V_{ex}.

Details on measurement setup, modeling, and eddy covariance analysis are found in the Supporting Information S1 [*Junninen et al*., 2010; *Kaimal and Finnigan*, 1994].

3. Results and Discussion

3.1. Overview

HCOOH concentrations, fluxes, and V_{ex} for the duration of the campaign (local time, i.e., UTC + 3), and meteorological parameters are displayed in Figure 1. Formic acid concentrations [HCOOH] varied from <0.05 to >3 ppbv, highest during relatively warm periods, and lowest during relatively cold, dark, and rainy periods. Levels exceeded 1 ppbv only with air temperature >20°C. Precipitation events usually brought about a decrease in [HCOOH]. The range of concentrations observed agrees well with previous measurements made using different techniques at the same site above the canopy (0.26 to 2.5 ppbv, in August 2001) [*Boy et al*., 2004]. Measurements in other places have also been of the same general order [*Seco et al*., 2007].

The *net flux* of HCOOH was mostly upward; the campaign average (± standard deviation) midday V_{ex} was $+0.7 \pm 1.7$ cm s^{-1}. This observation is remarkable, as measurements elsewhere have reported bidirectional, but mainly downward fluxes for HCOOH; e.g., a typical downward exchange at -0.2 cm s^{-1} over the Amazon during the wet season [*Kuhn et al*., 2002] or a midday average V_{ex} of -1 ± 0.4 cm s^{-1} over a southeastern U.S. forest in June/July [*Nguyen et al*., 2015]. The upward HCOOH V_{ex} we measured mostly occurred during bright days (Figure 1 and Supporting Information S1), whereas periods of net downward exchange were usually associated with periods of high relative humidity (RH). Those humid periods occurred in conjunction with at least some precipitation within the preceding 12 h, suggesting that HCOOH deposition via uptake on wetted canopy elements was an important sink.

3.2. Flux Budget Analysis

To interpret our flux measurements, we consider the elements of the mass balance equation:

$$F + \dot{S} = \int_0^h (P - L + E - D + T_{x,y})\,dz \quad (1)$$

Here F is the eddy flux of the respective compound, $\dot{S}$ the compound's storage change flux below the measurement height h, P the chemical production rate, L the chemical loss rate, E the emission rate, D the deposition rate and $T_{x,y}$ the horizontal advection of the compound. The median storage change term for HCOOH was 0.013 ppbv cm s^{-1}, i.e., relatively small for most flux periods (Supporting Information S1), so we neglected $\dot{S}$ in the following. We also neglected $T_{x,y}$, as we assume a sufficiently homogeneous boreal forest environment around the measurement site and an absence of nearby point sources. The main chemical loss for HCOOH (L) is by reaction with OH, with a rate constant of 4.5×10^{-13} cm^3 molec^{-1} s^{-1} [*Atkinson et al*., 2006]. Typical daytime OH concentrations are 10^6 molec cm^{-3} in spring/summer [*Hens et al*., 2014], so $\int_0^h L\,dz$ is $<5 \times 10^{-3}$ ppbv cm s^{-1}, and also negligible. We thus define the sum of the net flux and deposition rate, $F + D$, as the "gross flux," F^*, that in theory is represented by the remaining terms in equation (1), P and E.

We parameterized D using a standard resistance model [e.g., *Wesely*, 1989], wherein HCOOH transport to surfaces and subsequent deposition are described by a set of resistances (R) (see Supporting Information S1) [*Cho et al*., 2012; *Seinfeld and Pandis*, 1998; *Zhang et al*., 2003]. If dry deposition caused *all* downward HCOOH exchange, the total conductance ($1/R_{tot}$) would present an upper limit for the measured deposition velocities ($-V_{ex}$). Indeed, $-V_{ex} \leq 1/R_{tot}$ within uncertainties throughout the campaign. We illustrate the relation between measured $-V_{ex}$ and our estimates of the deposition-limiting resistances for a period of four consecutive days in Figure 2. Only on one of these days is the net HCOOH exchange mainly downward (i.e., $-V_{ex} > 0$), coinciding with a period of high RH and, in this case, some light rain (0.12 mm h^{-1}), as was typical (e.g., Figure 1).

Direct emissions E of HCOOH by plants and soil are estimated following parameterizations used by *Paulot et al*. [2011]. Vegetative emissions E_{veg} are computed using the parameterized canopy environment emission activity (PCEEA) algorithm developed for the Model of Emissions of Gases and Aerosols from Nature (MEGAN) [*Guenther*, 2007; *Guenther et al*., 2006; *Millet et al*., 2010] We added an estimate for soil emissions also following *Paulot et al*. [2011]. Other direct sources (e.g., ants) are estimated small or poorly understood and thus ignored. Further discussion is provided in the Supporting Information S1 [*Guenther et al*., 2012; *Pilegaard et al*., 2006; *Punttila*, 1996; *Rinne et al*., 2007]. The sum of these plant and soil HCOOH emissions is about an order of magnitude below the F^* we derive from our observations (Figure 3).

Chemical production (P) from VOC oxidation is a major global source of HCOOH. Using the GEOS-Chem model, *Millet et al*. [2015] predict that in the Finnish boreal forests, more than half of HCOOH originates from photochemical production, most likely via monoterpene oxidation ($C_{10}H_{16}$) [*Rinne et al*., 2009; *Tarvainen et al*., 2005, 2007]. To assess the influence of near-field chemical production on measured HCOOH fluxes, we employed the 1-D chemical transport model SOSAA (Simulate Organic vapors, Sulphuric Acid and Aerosols) [*Boy et al*., 2011; *Smolander et al*., 2014; *Zhou et al*., 2014] (details in the Supporting Information S1). The chemical precursors of HCOOH in SOSAA are β-pinene, limonene, isoprene, β-caryophyllene, and 2-methyl-3-buten-2-ol (MBO) [*Carrasco et al*., 2007]. However, nonzero HCOOH yields have been reported from oxidation of other terpenes [e.g., *Larsen et al*., 2001; *Lee et al*., 2006a, 2006b], including α-pinene and Δ3-carene, which

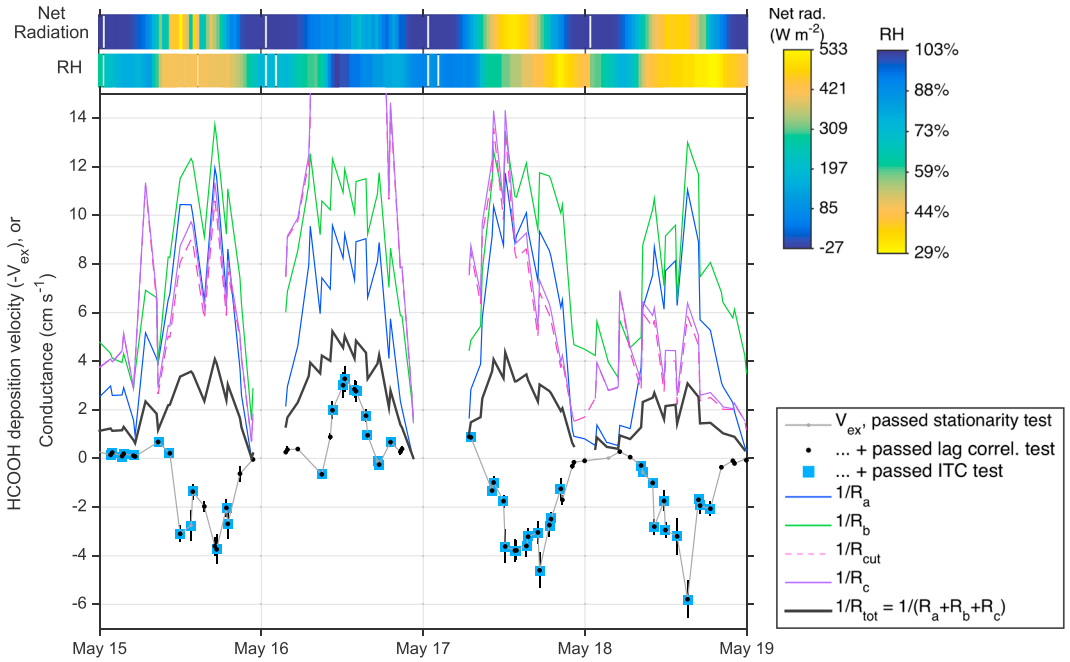

Figure 2. HCOOH deposition velocity ($-V_{ex}$; same symbol coding as Figure 1) for four selected days, together with estimates for conductances (inverse of resistances) that govern HCOOH dry deposition: the aerodynamic conductance ($1/R_a$), the laminar sublayer conductance ($1/R_b$), and the cuticular conductance ($1/R_{cut}$), which mostly controlled the residual conductance ($1/R_c$). The total conductance ($1/R_{tot}$), black line, represents the upper limit deposition velocity. Off-scale values for $1/R_{cut}$ (~160 cm s^{-1}, 16 May at noon) are due to high RH and precipitation. Color series on top of the main plot illustrates radiation conditions (e.g., thick clouds on 16 May, cloud-free on 17 May) and RH.

are emitted in largest quantities at SMEAR II [*Bäck et al.*, 2012]. To obtain a more general (and higher) estimate of potential HCOOH chemical sources, we assume HCOOH is produced as a first-generation product from the reaction of *any* terpene with OH or O_3, at literature-based yields (see Supporting Information S1). Integrating the resulting vertical profiles of HCOOH production rates to the measurement height leads to a production flux P (equation (1)) 2 to 3 orders of magnitude smaller than our observationally derived gross flux F^* (Figure 3). The discrepancy can be reduced with the simpler assumption that 10% of the total monoterpene emission rate in SOSAA is immediately converted to HCOOH (purple in Figure 3). For that case, the maximum flux contribution is comparable to the expected HCOOH direct emissions (brown in Figure 3), i.e., still about 1 order of magnitude lower than required to explain F^*. Altogether, these comparisons strongly suggest that prompt sources of atmospheric HCOOH above a boreal forest are much larger than current understanding would suggest.

Despite the failure of the above parameterizations to quantitatively explain F^*, there is clear temporal correlation between F^* and the parameterizations for either a direct emission source or a prompt chemical transformation of biogenic VOC, suggesting that the missing HCOOH source is tied to general ecosystem activity (Figures 3 and S7). This finding agrees with previous studies. *Nguyen et al.* [2015] measured eddy fluxes of HCOOH over a southeastern U.S. forest during summer and determined midday average net deposition at 1 ± 0.4 cm s^{-1}. However, that was about half of the deposition velocity predicted from resistance modeling, a discrepancy that suggested a daytime canopy emission flux of ~1 nmol m^{-2} s^{-1}, i.e., of the same order as our F^*. They suggested in-canopy secondary chemical pathways as the main source of HCOOH. *Millet et al.* [2015] compared chemical transport model predictions with a comprehensive set of observations in the isoprene-rich U.S. southeast. They found that either a 3-fold increase in the model's HCOOH yield from isoprene oxidation or a 26-fold increase in the model's direct emissions was required to fit some of their observations. *Stavrakou et al.* [2012] found similar discrepancies between a global-scale chemical model and satellite measurements of HCOOH columns. They predicted a substantial biogenic source of HCOOH of about 90 Tg yr^{-1} globally, as opposed to 25 Tg yr^{-1} in their standard model simulation, and suggested unidentified HCOOH formation pathways from the photochemical degradation of terpenoids as the most likely major missing source.

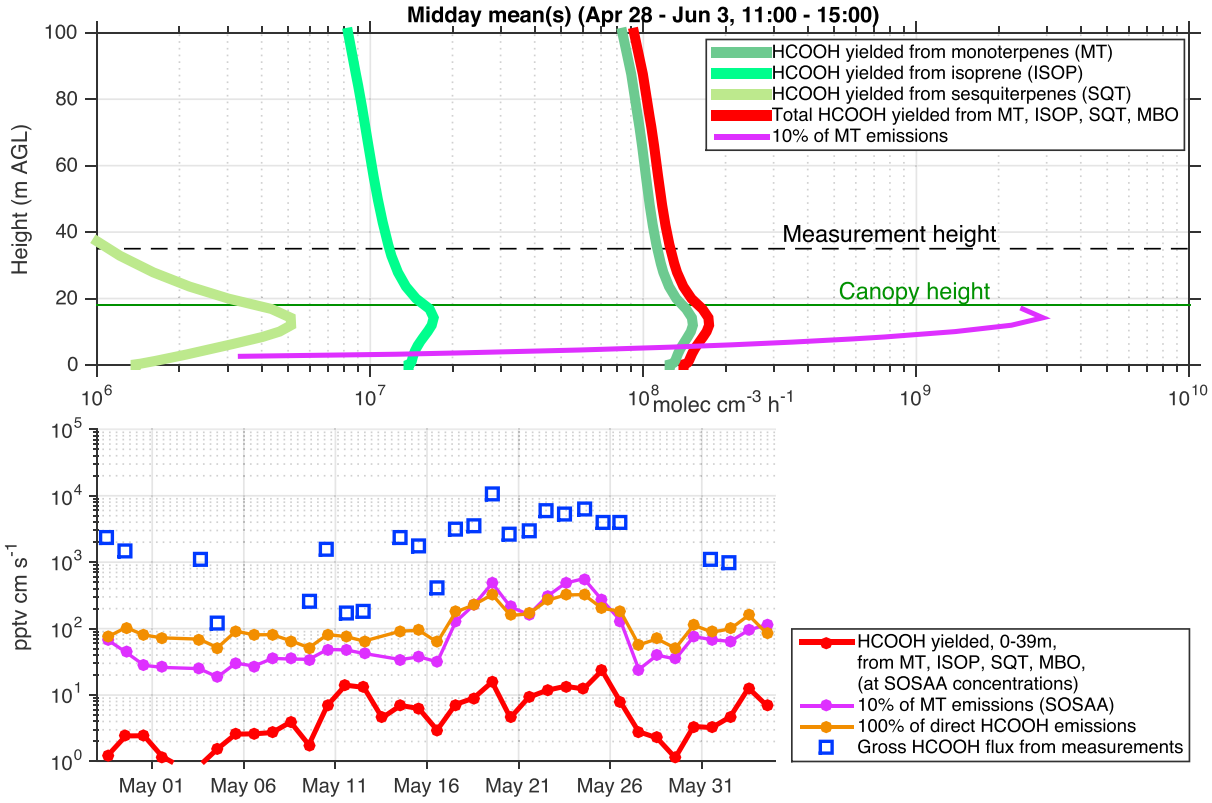

Figure 3. (top) Vertical profiles of HCOOH production rates from VOC reactions (shades of green), and the total HCOOH production rate (red), in units of molecules $cm^{-3}\,h^{-1}$. Profiles are midday (11:00 to 15:00, local time, UTC + 3) means over the campaign, calculated using SOSAA model output (see text). The purple profile represents 10% of the SOSAA total monoterpene emission rate. (bottom) Midday mean HCOOH fluxes obtained by integrating production rates (Figure 3, top) up to 39 m (red), 10% of the total monoterpene emission flux (purple), literature-based direct HCOOH emission flux (brown), and *F** derived from our measurements (blue squares; using only midday data and the highest quality flux periods as shown by squares in Figures 1 and 2; in units of parts per trillion by volume, pptv, cm s^{-1}).

3.3. Implied HCOOH Production and Regional to Global Context

To put our measured upward HCOOH fluxes into a broader context, we linearly scaled the HCOOH and monoterpene emission parameterizations to fit the derived daytime gross fluxes. The best fit was achieved by scaling the standard plant HCOOH emission potential to 600 $\mu g\,m^{-2}\,h^{-1}$ (i.e., 20 times the standard model value) plus 50% of the monoterpene emission rate to represent prompt chemical production or direct emissions similar to monoterpenes. The mean total HCOOH source was 78 $\mu g\,m^{-2}\,h^{-1}$ for our measurement period (see Supporting Information S1). To test how such an increased HCOOH production would manifest in the regional to global atmosphere, we stepwise implemented those assumptions into the GEOS-Chem chemical transport model [*Chaliyakunnel et al.*, 2016] (see Supporting Information S1 for details): A base scenario used standard HCOOH sources; scenario 2 assumed an HCOOH emission potential of 600 $\mu g\,m^{-2}\,h^{-1}$ and an additional source of 50% of the monoterpene emission rate only for needleleaf and shrub plant functional types (PFT); scenario 3 extended that assumption to all nontropical plants except grasses and crops; scenario 4 extended it to all PFT.

In Figure 4, the corresponding model sensitivity runs are compared to observations from the Tropospheric Emission Spectrometer (TES; see Supporting Information S1 for details) [*Cady-Pereira et al.*, 2014; *Shephard et al.*, 2015] aboard NASA's Aura satellite, and to in situ measurements from the NOAA P-3 aircraft during the Southeast Nexus campaign (SENEX) (http://www.esrl.noaa.gov/csd/projects/senex/) [*Lee et al.*, 2014]. When comparing the GEOS-Chem results to TES observations, changes in overall agreement across the model scenarios were subtle and depended on location (Figure 4b versus 4c). The large model bias for the African tropics disappeared in scenario 4, whereas mixing ratios over boreal forest regions were still substantially underpredicted. These large remaining discrepancies are likely because the TES sensitivity peaks around 800 hPa, i.e., above the boundary layer where the HCOOH increases implemented here mainly manifest.

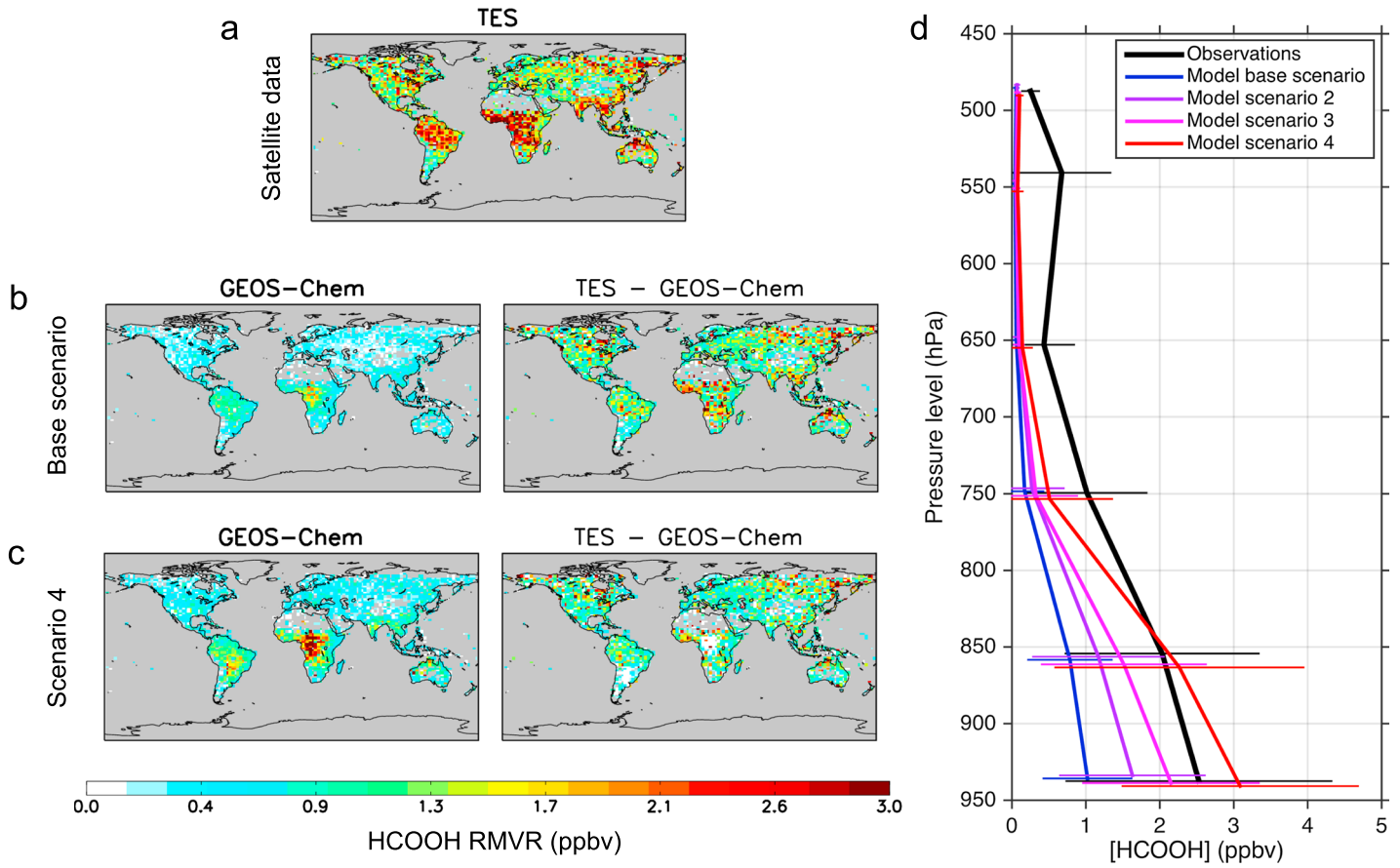

Figure 4. (a) Representative volume mixing ratio (see Supporting Information) of HCOOH, as determined using the satellite−based Tropospheric Emission Spectrometer (TES). (b) GEOS-Chem predictions sampled according to the TES sensitivity (left), and the difference from the satellite measurements (right). (c) Same as Figure 4b but for scenario 4, i.e., updated HCOOH emissions applied to all plant functional types. (d) Mean vertical profile of HCOOH mixing ratio measured by aircraft over the U.S. southeast during summer 2013 (black) [*Millet et al.*, 2015] and the corresponding GEOS-Chem predictions (see text for details).

Consistent with this idea, the discrepancy between the aircraft measurements of [HCOOH] and model predictions was substantially reduced within the boundary layer (< ~1 km altitude, Figure 4d), with the base scenario's 150% bias reduced to 55% (scenario 2) and 18% (scenario 3). Scenario 4 led to even slightly higher values near the surface than observed. In all cases, however, the large relative bias in the free troposphere remains unresolved.

These comparisons suggest that underestimated direct emissions and/or a fast high-yield chemical production from monoterpenes (or related compounds), supported by our observations of persistent upward fluxes of HCOOH over a boreal forest, can explain a significant fraction of high HCOOH mixing ratios routinely observed in the boundary layer over other forested regions. Scenarios 3 and 4 above are obviously upper limit extensions of our findings, and direct measurements of HCOOH emissions from various species of vegetation are needed. Free tropospheric mixing ratios still require a hitherto unaccounted-for chemical source of HCOOH.

4. Conclusions

Our direct flux observations suggest that large near-surface sources of HCOOH are missing and that these sources are biogenic with light and temperature dependences similar to existing emission parameterizations for many biogenic VOC. Both missing direct and secondary sources are plausible, due to gaps in our understanding of underlying processes, but the magnitude required makes standard gas-phase photochemical production from known precursors less likely. These findings corroborate earlier suggestions of near-surface sources of HCOOH that are currently missing in emission inventories and VOC degradation schemes.

However, even when applying model modifications to include such near-surface sources, strong [HCOOH] biases remain for the upper troposphere [*Millet et al*., 2015]. Moreover, fully reconciling observed and predicted HCOOH in the atmospheric boundary layer with surface emissions required much higher HCOOH emissions from all plant functional types than currently used. This hypothesis should be tested with direct measurement of species-specific HCOOH emissions from relevant tree species, as well as ground vegetation, litter, decaying plants, soil, and fauna. Ideally, such measurements are able to capture both direct emissions and a potential fast secondary production from short-lived VOC or surface-adsorbed oxidation products, which will require attention to losses of precursors and HCOOH to surfaces of the sampling apparatus. Eddy covariance provides a way to minimize such issues in a net-integrated sense, and with careful choice of fetch, could improve our understanding of species-specific emissions.

Acknowledgments

We thank T. Vesala, P. Kolari, P. Keronen, E. Siivola, M. Kajos, and A. Manninen at U. Helsinki for helpful discussions and model and measurement data related to SMEAR II. We also thank J. de Gouw (NOAA ESRL), and the SENEX and TES science teams for providing observations, and P. Punttila (Ympäristö) and D.M. Sorger (NC State) for entomological insights. The University of Washington participated in the BAECC campaign with funds from the U.S. Department of Energy (DE-SC0006867). S. Schobesberger acknowledges support from the European Commission (OXFLUX, project 701958), D. Taipale from the European Regional Development Fund (Centre of Excellence EcolChange), and D. B. M. from NSF CAREER (1148951) and the Minnesota Supercomputing Institute. We thank K. Cady-Pereira (AER), M. Shephard (Environment Canada), and M. Luo (JPL) for developing TES HCOOH measurements, publicly available at http://tes.jpl.nasa.gov/data/. GEOS-Chem model code is available at www.geos-chem.org. SOSAA model output, the high-frequency HCOOH mixing ratio measurements by CIMS, and anemometer wind measurements are available at http://hdl.handle.net/1773/36867.

References

Atkinson, R., D. L. Baulch, R. A. Cox, J. N. Crowley, R. F. Hampson, R. G. Hynes, M. E. Jenkin, M. J. Rossi, J. Troe, and I. Subcommittee (2006), Evaluated kinetic and photochemical data for atmospheric chemistry: Volume II—Gas phase reactions of organic species, *Atmos. Chem. Phys.*, *6*(11), 3625–4055.

Bäck, J., J. Aalto, M. Henriksson, H. Hakola, Q. He, and M. Boy (2012), Chemodiversity of a Scots pine stand and implications for terpene air concentrations, *Biogeosciences*, *9*(2), 689–702.

Boy, M., et al. (2004), Overview of the field measurement campaign in Hyytiälä, August 2001 in the framework of the EU project OSOA, *Atmos. Chem. Phys.*, *4*(3), 657–678.

Boy, M., A. Sogachev, J. Lauros, L. Zhou, A. Guenther, and S. Smolander (2011), SOSA—A new model to simulate the concentrations of organic vapours and sulphuric acid inside the ABL—Part 1: Model description and initial evaluation, *Atmos. Chem. Phys.*, *11*(1), 43–51.

Cady-Pereira, K. E., S. Chaliyakunnel, M. W. Shephard, D. B. Millet, M. Luo, and K. C. Wells (2014), HCOOH measurements from space: TES retrieval algorithm and observed global distribution, *Atmos. Meas. Tech.*, *7*(7), 2297–2311.

Carrasco, N., J. F. Doussin, M. O'Connor, J. C. Wenger, B. Picquet-Varrault, R. Durand-Jolibois, and P. Carlier (2007), Simulation chamber studies of the atmospheric oxidation of 2-methyl-3-buten-2-ol: Reaction with hydroxyl radicals and ozone under a variety of conditions, *J. Atmos. Chem.*, *56*(1), 33–55.

Chaliyakunnel, S., D. B. Millet, K. C. Wells, K. E. Cady-Pereira, and M. W. Shephard (2016), A large underestimate of formic acid from tropical fires: Constraints from space-borne measurements, *Environ. Sci. Technol.*, *50*(11), 5631–5640.

Cho, J., S. Miyazaki, P. J. Yeh, W. Kim, S. Kanae, and T. Oki (2012), Testing the hypothesis on the relationship between aerodynamic roughness length and albedo using vegetation structure parameters, *Int. J. Biometeorol.*, *56*(2), 411–418.

Duursma, R. A., et al. (2009), Contributions of climate, leaf area index and leaf physiology to variation in gross primary production of six coniferous forests across Europe: A model-based analysis, *Tree Physiol.*, *29*(5), 621–639.

Enders, G., et al. (1992), Biosphere/atmosphere interactions: Integrated research in a European coniferous forest ecosystem, *Atmos. Environ.*, *26A*(1), 171–189.

Farmer, D. K., P. J. Wooldridge, and R. C. Cohen (2006), Application of thermal-dissociation laser induced fluorescence (TD-LIF) to measurement of HNO_3, Σalkyl nitrates, Σperoxy nitrates, and NO_2 fluxes using eddy covariance, *Atmos. Chem. Phys.*, *6*(11), 3471–3486.

Foken, T., and B. Wichura (1996), Tools for quality assessment of surface-based flux measurements, *Agric. For. Meteorol.*, *78*(1–2), 83–105.

Glasius, M., et al. (2001), Relative contribution of biogenic and anthropogenic sources to formic and acetic acids in the atmospheric boundary layer, *J. Geophys. Res.*, *106*, 7415–7426.

Goode, J. G., R. J. Yokelson, D. E. Ward, R. A. Susott, R. E. Babbitt, M. A. Davies, and W. M. Hao (2000), Measurements of excess O_3, CO_2, CO, CH_4, C_2H_4, C_2H_2, HCN, NO, NH_3, HCOOH, CH_3COOH, HCHO, and CH_3OH in 1997 Alaskan biomass burning plumes by airborne Fourier transform infrared spectroscopy (AFTIR), *J. Geophys. Res.*, *105*, 22,147–22,166.

Graedel, T. E., and T. Eisner (1988), Atmospheric formic acid from formicine ants: A preliminary assessment, *Tellus, Ser. B*, *40B*(5), 335–339.

Guenther, A. B. (2007), Corrigendum to "Estimates of global terrestrial isoprene emissions using MEGAN (Model of Emissions of Gases and Aerosols from Nature)" published in Atmos. Chem. Phys., 6, 3181–3210, 2006, *Atmos. Chem. Phys.*, *7*(16), 4327.

Guenther, A. B., et al. (1995), A global model of natural volatile organic compound emissions, *J. Geophys. Res.*, *100*, 8873–8892, doi:10.1029/94JD02950.

Guenther, A. B., T. Karl, P. Harley, C. Wiedinmyer, P. I. Palmer, and C. Geron (2006), Estimates of global terrestrial isoprene emissions using MEGAN (Model of Emissions of Gases and Aerosols from Nature), *Atmos. Chem. Phys.*, *6*(11), 3181–3210.

Guenther, A. B., X. Jiang, C. L. Heald, T. Sakulyanontvittaya, T. Duhl, L. K. Emmons, and X. Wang (2012), The Model of Emissions of Gases and Aerosols from Nature version 2.1 (MEGAN2.1): An extended and updated framework for modeling biogenic emissions, *Geosci. Model Dev.*, *5*(6), 1471–1492.

Hari, P., and M. Kulmala (2005), Station for Measuring Ecosystem–Atmosphere Relations (SMEAR II), *Boreal Environ. Res.*, *10*, 315–322.

Hartmann, W. R., M. Santana, M. Hermoso, M. O. Andreae, and E. Sanhueza (1991), Diurnal cycles of formic and acetic acids in the northern part of the Guayana shield, Venezuela, *J. Atmos. Chem.*, *13*(1), 63–72.

Hens, K., et al. (2014), Observation and modelling of HO_x radicals in a boreal forest, *Atmos. Chem. Phys.*, *14*(16), 8723–8747.

Hofmann, U., D. Weller, C. Ammann, E. Jork, and J. Kesselmeier (1997), Cryogenic trapping of atmospheric organic acids under laboratory and field conditions, *Atmos. Environ.*, *31*(9), 1275–1284.

Jacob, D. J. (1986), Chemistry of OH in remote clouds and its role in the production of formic acid and peroxymonosulfate, *J. Geophys. Res.*, *91*, 9807–9826, doi:10.1029/JD091iD09p09807.

Junninen, H., A. Lauri, P. Keronen, P. Aalto, V. Hiltunen, P. Hari, and M. Kulmala (2009), Smart-SMEAR: On-line data exploration and visualization tool for SMEAR stations, *Boreal Environ. Res.*, *14*, 447–457.

Junninen, H., et al. (2010), A high-resolution mass spectrometer to measure atmospheric ion composition, *Atmos. Meas. Tech.*, *3*(4), 1039–1053.

Kaimal, J. C., and J. J. Finnigan (1994), *Atmospheric Boundary Layer Flows: Their Structure and Measurement*, Oxford Univ. Press, New York.

Kawamura, K., L. L. Ng, and I. R. Kaplan (1985), Determination of organic acids (C1–C10) in the atmosphere, motor exhausts, and engine oils, *Environ. Sci. Technol.*, *19*(11), 1082–1086.

Keene, W. C., J. N. Galloway, and J. D. Holden (1983), Measurement of weak organic acidity in precipitation from remote areas of the world, *J. Geophys. Res.*, *88*, 5122–5130, doi:10.1029/JC088iC09p05122.
Kesselmeier, J. (2001), Exchange of short-chain oxygenated Volatile Organic Compounds (VOCs) between plants and the atmosphere: A compilation of field and laboratory studies, *J. Atmos. Chem.*, *39*(3), 219–233.
Kesselmeier, J., et al. (1997), Emission of short chained organic acids, aldehydes and monoterpenes from *Quercus ilex* L. and *Pinus pinea* L. in relation to physiological activities, carbon budget and emission algorithms, *Atmos. Environ.*, *31*(Suppl. 1), 119–133.
Kesselmeier, J., K. Bode, C. Gerlach, and E. M. Jork (1998), Exchange of atmospheric formic and acetic acids with trees and crop plants under controlled chamber and purified air conditions, *Atmos. Environ.*, *32*(10), 1765–1775.
Kuhn, U., S. Rottenberger, T. Biesenthal, C. Ammann, A. Wolf, G. Schebeske, S. T. Oliva, T. M. Tavares, and J. Kesselmeier (2002), Exchange of short-chain monocarboxylic acids by vegetation at a remote tropical forest site in Amazonia, *J. Geophys. Res.*, *107*(D20), 8069, doi:10.1029/2000JD000303.
Kulmala, M., A. Laaksonen, P. Korhonen, T. Vesala, T. Ahonen, and J. C. Barrett (1993), The effect of atmospheric nitric acid vapor on cloud condensation nucleus activation, *J. Geophys. Res.*, *98*, 22,949–22,958, doi:10.1029/93JD02070.
Kulmala, M., et al. (2001), Overview of the international project on biogenic aerosol formation in the boreal forest (BIOFOR), *Tellus, Ser. B*, *53*(4), 324–343.
Larsen, B. R., D. Di Bella, M. Glasius, R. Winterhalter, N. Jensen, and J. Hjorth (2001), Gas-phase OH oxidation of monoterpenes: Gaseous and particulate products, *J. Atmos. Chem.*, *38*(3), 231–276.
Lee, A., A. H. Goldstein, J. H. Kroll, N. L. Ng, V. Varutbangkul, R. C. Flagan, and J. H. Seinfeld (2006a), Gas-phase products and secondary aerosol yields from the photooxidation of 16 different terpenes, *J. Geophys. Res.*, *111*, D17305, doi:10.1029/2006JD007050.
Lee, A., A. H. Goldstein, M. D. Keywood, S. Gao, V. Varutbangkul, R. Bahreini, N. L. Ng, R. C. Flagan, and J. H. Seinfeld (2006b), Gas-phase products and secondary aerosol yields from the ozonolysis of ten different terpenes, *J. Geophys. Res.*, *111*, D07302, doi:10.1029/2005JD006437.
Lee, B. H., F. D. Lopez-Hilfiker, C. Mohr, T. Kurtén, D. R. Worsnop, and J. A. Thornton (2014), An iodide-adduct high-resolution time-of-flight chemical-ionization mass spectrometer: Application to atmospheric inorganic and organic compounds, *Environ. Sci. Technol.*, *48*(11), 6309–6317.
Lopez-Hilfiker, F. D., et al. (2014), A novel method for online analysis of gas and particle composition: Description and evaluation of a Filter Inlet for Gases and AEROsols (FIGAERO), *Atmos. Meas. Tech.*, *7*(4), 983–1001.
Millet, D. B., et al. (2010), Global atmospheric budget of acetaldehyde: 3-D model analysis and constraints from in-situ and satellite observations, *Atmos. Chem. Phys.*, *10*(7), 3405–3425.
Millet, D. B., et al. (2015), A large and ubiquitous source of atmospheric formic acid, *Atmos. Chem. Phys.*, *15*(11), 6283–6304.
Nenes, A., R. J. Charlson, M. C. Facchini, M. Kulmala, A. Laaksonen, and J. H. Seinfeld (2002), Can chemical effects on cloud droplet number rival the first indirect effect?, *Geophys. Res. Lett.*, *29*(17), 1848, doi:10.1029/2002GL015295.
Nguyen, T. B., J. D. Crounse, A. P. Teng, J. M. S. Clair, F. Paulot, G. M. Wolfe, and P. O. Wennberg (2015), Rapid deposition of oxidized biogenic compounds to a temperate forest, *Proc. Natl. Acad. Sci. U.S.A.*, *112*(5), E392–E401.
Ngwabie, N. M., G. W. Schade, T. G. Custer, S. Linke, and T. Hinz (2008), Abundances and flux estimates of volatile organic compounds from a dairy cowshed in Germany, *J. Environ. Qual.*, *37*(2), 565–573.
Paulot, F., et al. (2011), Importance of secondary sources in the atmospheric budgets of formic and acetic acids, *Atmos. Chem. Phys.*, *11*(5), 1989–2013.
Pilegaard, K., et al. (2006), Factors controlling regional differences in forest soil emission of nitrogen oxides (NO and N_2O), *Biogeosciences*, *3*(4), 651–661.
Punttila, P. (1996), Succession, forest fragmentation, and the distribution of wood ants, *Oikos*, *75*(2), 291–298.
Rannik, Ü., T. Markkanen, J. Raittila, P. Hari, and T. Vesala (2003), Turbulence statistics inside and over forest: Influence of footprint prediction, *Boundary Layer Meteorol.*, *109*, 163–189.
Rinne, J., R. Taipale, T. Markkanen, T. M. Ruuskanen, H. Hellén, M. K. Kajos, T. Vesala, and M. Kulmala (2007), Hydrocarbon fluxes above a Scots pine forest canopy: Measurements and modeling, *Atmos. Chem. Phys.*, *7*(12), 3361–3372.
Rinne, J., J. Bäck, and H. Hakola (2009), Biogenic volatile organic compound emissions from the Eurasian taiga: Current knowledge and future directions, *Boreal Environ. Res.*, *14*, 807–826.
Sander, R. (2015), Compilation of Henry's law constants (version 4.0) for water as solvent, *Atmos. Chem. Phys.*, *15*(8), 4399–4981.
Sanhueza, E., and M. O. Andreae (1991), Emission of formic and acetic acids from tropical savanna soils, *Geophys. Res. Lett.*, *18*, 1707–1710, doi:10.1029/91GL01565.
Schuepp, P., M. Leclerc, J. MacPherson, and R. Desjardins (1990), Footprint predictions of scalar fluxes from analytical solutions of the diffusion equation, *Boundary Layer Meteorol.*, *50*, 355–373.
Seco, R., J. Peñuelas, and I. Filella (2007), Short-chain oxygenated VOCs: Emission and uptake by plants and atmospheric sources, sinks, and concentrations, *Atmos. Environ.*, *41*(12), 2477–2499.
Seinfeld, J. H., and S. N. Pandis (1998), *Atmospheric Chemistry and Physics: From Air Pollution to Climate Change*, John Wiley, New York.
Shephard, M. W., et al. (2015), Tropospheric Emission Spectrometer (TES) satellite validations of ammonia, methanol, formic acid, and carbon monoxide over the Canadian oil sands, *Atmos. Meas. Tech.*, *8*(12), 9503–9563.
Smolander, S., et al. (2014), Comparing three vegetation monoterpene emission models to measured gas concentrations with a model of meteorology, air chemistry and chemical transport, *Biogeosciences*, *11*(19), 5425–5443.
Stavrakou, T., et al. (2012), Satellite evidence for a large source of formic acid from boreal and tropical forests, *Nat. Geosci.*, *5*(1), 26–30.
Suzuki, Y. (1997), Automated analysis of low-molecular weight organic acids in ambient air by a microporous tube diffusion scrubber system coupled to ion chromatography, *Anal. Chim. Acta*, *353*(2–3), 227–237.
Talbot, R. W., K. M. Beecher, R. C. Harriss, and W. R. Cofer (1988), Atmospheric geochemistry of formic and acetic acids at a mid-latitude temperate site, *J. Geophys. Res.*, *93*, 1638–1652, doi:10.1029/JD093iD02p01638.
Tarvainen, V., H. Hakola, H. Hellén, J. Bäck, P. Hari, and M. Kulmala (2005), Temperature and light dependence of the VOC emissions of Scots pine, *Atmos. Chem. Phys.*, *5*(4), 989–998.
Tarvainen, V., H. Hakola, J. Rinne, H. Hellén, and S. Haapanala (2007), Towards a comprehensive emission inventory of terpenoids from boreal ecosystems, *Tellus, Ser. B*, *59*(3), 526–534.
Vesala, T., et al. (2005), Effect of thinning on surface fluxes in a boreal forest, *Global Biogeochem. Cycles*, *19*, GB2001, doi:10.1029/2004GB002316.
Wesely, M. L. (1989), Parameterization of surface resistances to gaseous dry deposition in regional-scale numerical models, *Atmos. Environ.*, *23*(6), 1293–1304.

Wolfe, G. M., J. A. Thornton, R. L. N. Yatavelli, M. McKay, A. H. Goldstein, B. LaFranchi, K. E. Min, and R. C. Cohen (2009), Eddy covariance fluxes of acyl peroxy nitrates (PAN, PPN and MPAN) above a Ponderosa pine forest, *Atmos. Chem. Phys.*, *9*(2), 615–634.

Yuan, B., et al. (2015), Investigation of secondary formation of formic acid: Urban environment vs. oil and gas producing region, *Atmos. Chem. Phys.*, *15*(4), 1975–1993.

Zhang, L., J. R. Brook, and R. Vet (2003), A revised parameterization for gaseous dry deposition in air-quality models, *Atmos. Chem. Phys.*, *3*(6), 2067–2082.

Zhou, L., T. Nieminen, D. Mogensen, S. Smolander, A. Rusanen, M. Kulmala, and M. Boy (2014), SOSAA—A new model to simulate the concentrations of organic vapours, sulphuric acid and aerosols inside the ABL—Part 2: Aerosol dynamics and one case study at a boreal forest site, *Boreal Environ. Res.*, *19*(suppl. B), 237–256.